Power-law photoconductivity time decay in nanocrystalline TiO_2 thin films

2007 J. Phys.: Condens. Matter 19 486205

(http://iopscience.iop.org/0953-8984/19/48/486205)

IOP PUBLISHING JOURNAL OF PHYSICS: CONDENSED MATTER

J. Phys.: Condens. Matter **19** (2007) 486205 (10pp) doi:10.1088/0953-8984/19/48/486205

Power-law photoconductivity time decay in nanocrystalline TiO_2 thin films

D Comedi[1,2], S P Heluani[1], M Villafuerte[1,2], R D Arce[3] and R R Koropecki[3]

[1] Laboratorio de Física del Sólido, Departamento de Física, FACEyT, Universidad Nacional de Tucumán, Avenida Independencia 1800, 4000 Tucumán, Argentina
[2] Consejo Nacional de Investigaciones Científicas y Técnicas (CONICET), Argentina
[3] INTEC (CONICET-UNL), Güemes 3450, 3000 Santa Fe, Argentina

E-mail: dcomedi@herrera.unt.edu.ar

Received 27 August 2007, in final form 17 October 2007
Published 6 November 2007
Online at stacks.iop.org/JPhysCM/19/486205

Abstract

The sub-band-gap excited photoconductivity (PC) time decay and the film structure of rf-sputter deposited nanocrystalline TiO_2 thin films have been studied. Atomic force microscopy and x-ray diffraction measurements were used to assess roughness, crystalline structure and mean grain size of the films. Samples fabricated under different deposition conditions exhibit different microstructures and absolute PC, but similar persistent PC behaviour after switching off the light source. The very slow PC decay can be well represented by a function that is nearly constant for short times and decreases as a power law for times longer than about 100 s. This function is shown to be consistent with a rate equation characterized by a relaxation time that increases linearly with time. This behaviour, in turn, agrees with predictions of a previously reported model that assumes electron–hole recombination limited by carrier-density-dependent potential barriers associated with inhomogeneities. These results may have important implications on attempts to determine distributions of trap energies from PC decay curves in TiO_2.

(Some figures in this article are in colour only in the electronic version)

1. Introduction

Many important applications of TiO_2 thin films, such as in photo-electrochemical solar cells, photo-catalytic reactors for pollution control and chemical sensors, require a high surface area for enhancement of the active film contact with the surrounding medium [1]. One way of achieving this is by physical vapour deposition of films exhibiting high surface roughness. This can be done by choosing deposition conditions where the mobility of depositing atoms is

kinetically limited (i.e. by reducing the substrate temperature and/or increasing the deposition rate) [2]. Corresponding bulk structures, however, are usually heterogeneous, and small crystallites in distinct polymorphs can coexist with nanometric amorphous and low-density regions. Critical questions then naturally arise regarding the carrier transport mechanisms that apply in such structures, which are not only very relevant for the various technological applications of TiO_2 thin films, but also of timely fundamental interest. In recent years, intense theoretical and experimental activity aimed at the understanding of transport in disordered media has been carried out [3]. The measurement of photoconductivity (PC) decay has been one of the important characterization methods of charge transport in amorphous [4], organic solids [5], polymers [6] and polycrystalline [7, 8] semiconductors. In polycrystalline wide band gap oxide semiconductors such as ZnO and TiO_2, the PC has been observed to decay very slowly, over a period of many hours to several days [7–9]. This slow decay is often referred to as 'persistent PC' and different possible explanations have been proposed [4–10]. In some cases, models have been fitted to the experimental data for the determination of electronic parameters of the materials, such as the energy distribution of charge carrier traps [7, 8].

In this paper, we report on the sub-gap PC decay in rf-sputtered nanocrystalline TiO_x ($x \sim 2$) thin films prepared under different deposition conditions that lead to samples with various distinct structural properties. These samples exhibit interesting hysteretic current–voltage characteristics at sufficiently large voltages, indicative of a switching effect [11–13] and, as shown here, they present persistent PC behaviour. We find that the conductivity after the illumination is interrupted changes very little for short times and decays as a power law for longer times. This behaviour differs from results from TiO_2 thin films reported in the literature and is shown here to be consistent with a PC relaxation time that evolves linearly with time. This finding leads us to conclude that charge separation due to internal potential barriers due to inhomogeneities, which has been neglected in previous interpretations [7–9], may be an important determining factor of the PC decay profiles in nanocrystalline TiO_2.

2. Experimental details

Samples were reactively rf-sputtered TiO_x thin films (400–500 nm thickness) deposited onto commercial low-resistivity indium–tin-oxide (ITO) coated glass and Corning glass substrates. A 99.95% purity Ti target and mixtures of O_2 and Ar gases (5N purity) were used in the depositions (typical base pressure 2×10^{-7} mbar). The composition (O/Ti ratio or x in TiO_x) was determined by Rutherford backscattering measurements. Several Ag electrodes were vacuum deposited on the top of the thin films. A Keithley 617 electrometer was used to measure the current while polarizing the samples between one of the Ag and the bottom ITO electrodes with the built-in power source set at 0.1 V. This voltage (an applied field of about 2×10^3 V cm^{-1}) corresponds to the linear (ohmic) regime of the I–V curve, which bends upwards and becomes hysteretic for voltages above ∼0.3 V, indicating switching behaviour [13]. PC decay was studied in vacuum by measuring the current changes after excitation of the films through the transparent ITO electrode using two commercial light-emitting diodes (peak at $h\nu = 3.1$ eV and spectral definition ∼5%) as the light source. This photon energy is slightly lower than the TiO_2 band gap energies and hence films are illuminated thoroughly from the transparent ITO contact up to the Ag electrode. From the measured optical absorption coefficients and film thicknesses, we estimate that ∼10–14% of the incident photon flux is actually absorbed in the TiO_2 films. The samples were illuminated for 30–200 min (estimated flux density of ∼10 mW cm^{-2}) until the current had increased significantly but had not in general achieved saturation; then the light source was switched off at $t = 0$ for PC decay measurements in typically the $t = 0.5$–10 000 s range. The morphology of the

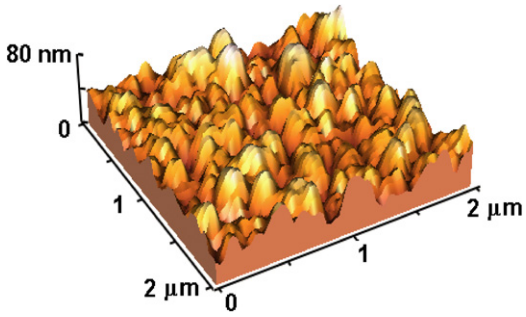

Figure 1. AFM image of sample S2.

Table 1. Relevant structural parameters (RMS roughness, anatase to rutile ratio and mean crystallite size) and band gap of the TiO_x films examined in this work.

TiO_x sample	$x(\pm 0.02)$	RMS roughness (nm)	Anatase to rutile ratio	Mean cryst. size (nm)	E_g (eV)
S1	2.04	6	5.5	37	3.34
S2	2.00	12	0.3	7	3.18

films was assessed through atomic force microscopy (AFM). The crystalline structure and mean crystallite size (c.s.) were determined from x-ray diffraction patterns, which showed peaks corresponding to the two main TiO_2 polymorphs, namely anatase and rutile. Optical parameters were obtained from optical transmittance measurements in the visible–UV range using a procedure outlined by Swanepoel [14]. The gap energy (E_g) was estimated from the relation $\alpha^{1/2} \propto h\nu - E_g$ (where α and $h\nu$ are the absorption coefficient and photon energy, respectively) corresponding to indirect transition, as expected for TiO_2 since direct transitions are dipole forbidden in this material [15].

3. Results

Two TiO_x samples (S1 and S2) with $x \sim 2$ were chosen here for a careful study of the PC decay. S1 was grown on heated (350 °C) substrates, while S2 was grown with no intentional heating of the substrates (some unintentional heating occurred as a result of bombardment of the growth surface by plasma and sputtered products). As expected, S1 exhibits larger crystallites and a smoother morphology as compared with S2. The main physical properties of both films are presented in table 1. It can be noted that substrate heating during growth also promotes the preferential formation of anatase in S1, while the deposition at the lower temperature leads to preferential formation of small rutile crystallites.

Figure 1 shows an AFM picture of S2. Large features of about 300 nm diameter can be seen on the surface, which are much larger than the mean c.s. of 7 nm. This kind of morphology is usually ascribed to the formation of non-coalescent islands during the first stages of the deposition followed by preferential growth on the top of the islands due to shadowing effects, leading to density-heterogeneous structures as expressed in Thornton's physical vapour deposition diagram for the low temperature growth regime [16]. Corresponding AFM images of S1, in contrast (not shown), reveal small features, of the same order as the corresponding c.s. of 37 nm, indicating that the morphology here is not limited by low adatom mobilities during deposition but by crystallite facets.

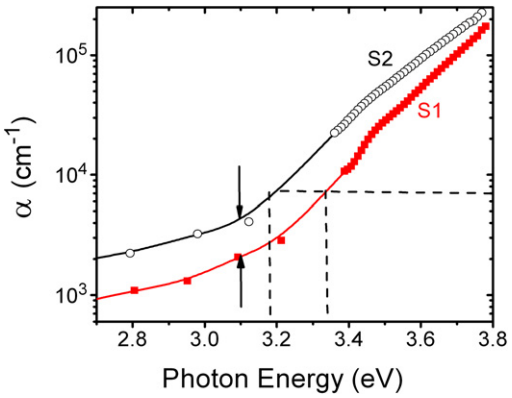

Figure 2. Absorption coefficient (α) as a function of the photon energy for samples S1 and S2. Solid lines through the data points are guides to the eye. The vertical dashed lines indicate the corresponding band gap energies for S1 and S2 (from table 1); the horizontal dashed line shows the corresponding α values (almost identical for both samples). Arrows indicate the photon energy used in the PC experiments.

Figure 2 shows the absorption coefficient as a function of the incident photon energy for samples S1 and S2. The red shift of the absorption edge for S2 with respect to that for S1 is mainly due to the expected smaller band gap of the rutile phase as compared to anatase [17]. S2, in addition, presents increased sub-gap absorption (between 2.7 and 3.1 eV), indicating a larger density of band gap states close to either the conduction or valence bands, or both. These levels are presumably due to disorder-induced (bond angle and length distortions) localized states and could also be disorder-broadened point defect levels (O vacancies or Ti interstitials [18, 19]) at grain boundaries. The broad absorption edges in figure 2 (between 3.1 and ∼3.5 eV) are consistent with exponential functions of energy with characteristic slopes of 0.12 eV (S1) and 0.15 eV (S2). Such large slopes are consistent with exponentially decaying density of localized state tails beyond the energy bands into the band gap. These have been reported for amorphous [20] and polycrystalline [21] semiconductors, including nanocrystalline TiO_2 films [22], and are usually ascribed to lattice disorder (strain) or to potential fluctuations due to charged states at point or grain boundary defects.

Figure 3 shows the electrical current measured in samples S1 and S2 after switching off the light source at $t = 0$. The dark current values for both samples are also shown for reference. Sample S1 is four times more resistive in the dark than S2 at room temperature, but it turns out to be about 3000 times more conductive than S2 when illuminated (note the break in the current scale in figure 3). The conduction in the dark at RT is dominated by phonon assisted variable range hopping between localized states near the Fermi energy [11, 12]. The slightly larger dark resistivity of S1 as compared to S2 is thought to be due to a reduced hopping probability resulting from a larger mean distance between hopping sites associated with the lower density of disorder-related states in this sample. It can also be seen in figure 3 that after the excitation has been switched off, the current changes very little for about 30–50 s, and then falls off very slowly for both S1 and S2. The current in S1 is a smooth function of time; that of S2, in turn, is somewhat noisy. It should be emphasized, however, that these fluctuations are well above the noise level of the measurement system.

In figure 4, the data of figure 3 have been replotted as the normalized PC decay profile, defined as $\Delta\sigma(t)/\Delta\sigma(0)$ and calculated by equating it to the normalized current difference, namely $[I(t) - I_{\text{dark}}]/[I(0) - I_{\text{dark}}]$. Despite the significant differences in microstructure

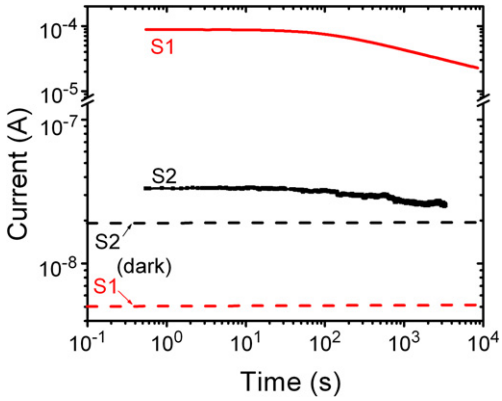

Figure 3. Current as a function of time for samples S1 and S2 at room temperature. The corresponding currents measured in the dark are shown for reference as horizontal dashed lines. The illumination duration was 1800 s and then the light source was turned off at $t = 0$. Note the break in the current scale.

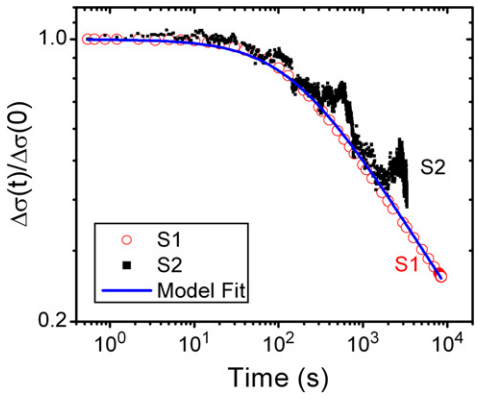

Figure 4. Photoconductivity normalized by its value just before switching off the light source at $t = 0$ for samples S1 and S2 as a function of time. The solid line is a model fit to the S1 data (equation (1)), as explained in section 4 in the text.

between S1 and S2, the overall decay profile is quite similar for both samples, except for the fluctuations observed for S2. Furthermore, it is clear from the linear dependence of the S1 data for $t > 100$ s that the PC relaxation obeys a power-law time decay.

4. Discussion

During sub-gap illumination, electrons and holes are readily promoted from localized band gap states into extended states in the conduction and valence bands and the conductivity increases. Many of these charges, however, will be rapidly captured by shallow traps and may eventually fall into deep traps. Conduction in these samples is n-type as it often is in TiO_2 due to the much lower hole mobility than electron mobility [23]. Electrons trapped in sub-gap states may be reemitted back to the band, and then the transport may be dispersive as described by the multiple trapping model [24], or within continuum random walk [25] theory. The equivalences and differences between these two approaches have been discussed recently [26]. The measured

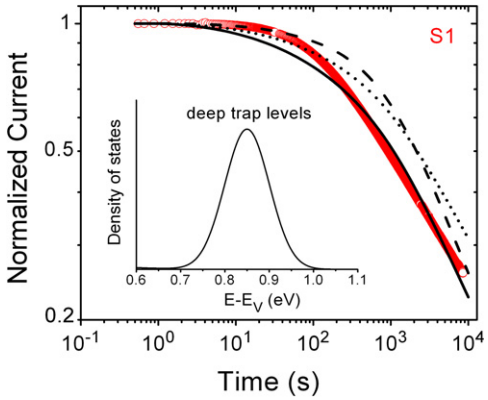

Figure 5. Current as a function of time for sample S1 (open circles, from figure 3) and results of calculations using a model [8] that assumes that current decay is essentially determined by thermal emission of holes from deep levels. The current values are normalized to their value at $t = 0$ to compare decay profiles. The deep level distribution (inset) was assumed to be a Gaussian (width = 0.07 eV) located at 0.85 eV (solid line) and 0.87 eV (dotted line). The dashed line corresponds to a Gaussian position and width of 0.87 and 0.03 eV, respectively.

conductivity after illumination should be determined by the effective density of electrons in conduction states and the effective mobility, which may be very different from the hopping mobility of carriers in the dark. Since the material is spatially inhomogeneous, however, it is expected that regions close to interfaces will have larger trap densities than others, and therefore they may exhibit space charge and potential barriers that could affect the conductivity locally.

The present PC decay experiments should be distinguished from photocarrier transients measured after short light pulse excitations [27]. Those transients occur for very short times and usually probe electron photocarrier transport within band tails before they can recombine. The power-law transients observed in such experiments are usually interpreted in terms of multiple trapping transport in an exponential band tail trap distribution. The time profile of slow PC decays studied here, in contrast, are expected to be dominated by electron–hole recombination processes. Previous studies of the PC decay in TiO_2 and ZnO have attributed it to slow thermal emission of holes from a broad energy distribution of hole traps deep in the band gap (which have been ascribed tentatively to O vacancies) [7, 8]. In this model, it is assumed that nonequilibrium holes are immediately trapped in these deep traps and therefore the excess electron density is equated to the density of trapped holes [7, 8]. The electron mobility is taken as constant and the PC decay is calculated from a rate equation describing the electron recombination with holes after the latter are thermally emitted back to the valence band. A more recent version of this model incorporates the effect of potential fluctuations due to charged interface states on trap energy levels and screening effects to explain an experimentally observed light intensity dependence of the PC relaxation [9]. The main result of these models is that the time profile of the PC decay is a function of the energy distribution of deep hole traps and this has been exploited to deduce this distribution from the experimental decay data [7, 8]. However, such models neglect effects of inhomogeneities such as grain boundary interface barriers and density fluctuations on carrier transport and recombination. Nevertheless, we have tried as a first approach to fit a simple version of these models to the PC decay profiles. This is shown for sample S1 in figure 5. Using a reasonable model density of states that includes a Gaussian broadened energy distribution of populated hole traps (inset of figure 5), and assuming an attempt to escape frequency of 10^{12} s^{-1}, the best fit is obtained when the hole

trap distribution is centred at 0.85 eV above the valence band. As can be seen in figure 5, the overall shape of the experimental data is correctly reproduced by the model. However, it fails to describe the detailed behaviour, as for instance the power-law decay clearly observed for $t > 100$ s. Indeed, the shape of the decay curve in this model is found to be very sensitive to the specific shape of the trap distribution function chosen and this is actually the basis of previous methods to deduce the distribution of trap energies from the experimental PC decay data.

One could possibly search for a certain trap distribution in an attempt to force the calculated curve to fit the power-law decay. However, we chose a different approach, for reasons that will become apparent below. The decay curves can be well fit by the function (see figure 4):

$$\Delta\sigma(t) = \Delta\sigma(0)(1 + bt)^{-\gamma}. \tag{1}$$

Such dependence is deliberately chosen to reproduce the power-law decay for long times and describes well most of the PC decay curves observed in this study. It is interesting to note that it can be obtained from a rate equation of the type:

$$\frac{\mathrm{d}\Delta\sigma}{\mathrm{d}t} = -\frac{\Delta\sigma}{\tau(t)}, \tag{2}$$

where

$$\tau(t) = \tau_0 + \frac{t}{\gamma} \tag{3}$$

with $\tau_0 = (b\gamma)^{-1}$. From the best fit shown in figure 4, we determine two independent parameters: $\tau_0 = 418$ s and $\gamma = 0.33$. A possible interpretation of this result is as follows: for short times $t \to 0$ most holes are still trapped in deep states and the recombination rate is very low, of the order of τ_0^{-1}. Indeed, assuming that τ_0 is limited by the mean hole thermal emission time from the deep levels to the valence band edge, we can estimate a corresponding energy level of:

$$E \approx k_{\mathrm{B}} T \ln(s\tau_0) = 0.87 \text{ eV} \tag{4}$$

(k_{B} is the Boltzmann constant, T the measurement temperature and $s \approx 10^{12}$ s^{-1} is the attempt-to-escape frequency) which is consistent with that estimated earlier for the deep hole trap distribution. For large $t \gg \gamma\tau_0$, the phenomenological relaxation time τ increases linearly as t/γ. A linearly time-dependent PC relaxation time was previously predicted by Sheinkman and Shlik (S–S) [10] who considered the influence of spatial inhomogeneities on carrier transport and recombination in disordered semiconductors. Their basic assumption in their simple model is that due to inhomogeneities, such as grain boundaries or low-density regions, internal electric fields (or potential barriers) exist in the material that spatially separate electrons and holes, thus inhibiting the recombination. As pointed out in [10], the extra charge injected by illumination tends to flatten down the bent bands at interfaces and hence the height of the potential barriers should be a decreasing function of the nonequilibrium charge carrier density. During relaxation, the carrier density decreases by recombination across the barriers, leading to a gradual recovery of the potential barriers and therefore to an increase of the recombination time. For the case of nanocrystalline TiO_2, it is expected that deep states due to defect complexes will preferentially occur at interfaces between crystallites. Trapping of holes in these states will obviously affect the space charge and hence the interfacial barrier heights. The slow thermal release of these holes would then still be the rate determining step at short times, as proposed in earlier models [7–9]. But here, in contrast, carriers are spatially separated and therefore need to surmount a time-dependent potential barrier before recombining. As time evolves, the barriers become higher and the recombination time increases linearly, as observed here and predicted by

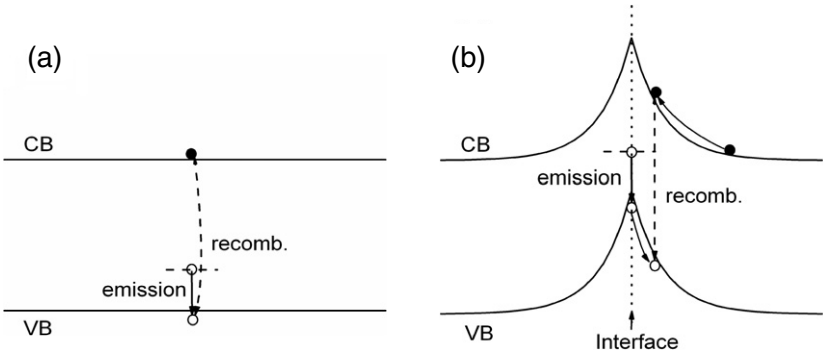

Figure 6. Schematic description of possible models for persistent PC in TiO_2. (a) Homogeneous TiO_2 model: bands are flat and recombination occurs immediately after thermal emission of a hole from a deep trap, (b) inhomogeneous TiO_2 model: band bending occurs due to trapped charge at interfaces between different regions (i.e. crystallites, amorphous or differing density). Holes and electrons are spatially separated and need to surmount a barrier after the hole has been emitted from the trap to recombine. The barrier becomes higher as recombination proceeds and the recombination time increases.

S–S [10]. A schematic representation of the situation is depicted in figures 6(a) and (b). This result indicates that care must be exercised when extracting trap distributions from PC time decay profiles. In the appendix, the relationship between equations (1)–(3) and the parameters from the S–S model is given.

It is somewhat striking that both PC data for S1 and S2 (figure 5) are consistent with practically the same deep hole trap energies with respect to the valence band edge despite their different microstructure (i.e. S2 is more rutile-like and has smaller crystallites and poorer morphology as compared to S1). Although the origin of hole traps in TiO_2 is still a matter of debate, it is well known that localized band gap states are created by high temperature reductions, showing that O vacancies or Ti interstitials are involved. Photoemission studies in TiO_2 thin films show that thermal reduction leads to band gap states at about the same energy with respect to the valence band edge in anatase and rutile [28], and there is supporting evidence to this result from luminescence measurements [29, 30]. This trend is consistent with a molecular-orbital picture [31] where the gross features of defect energetics are determined by the TiO_6 octahedral units that constitute both anatase and rutile TiO_2. Furthermore, random structural disorder should affect these states only indirectly (i.e. mostly broadening and little shifting). A trap distribution peaked at $\sim$0.85 eV, found to be consistent with our interpretation of the PC decay data, is in close agreement with values found in previous studies of TiO_2 and ZnO ($\sim$0.9 eV).

The next question to be addressed is the reason for the much lower absolute PC values observed for S2 as compared with S1. While the status of our study does not yet allow us to provide a definite explanation at present, few plausible possibilities can be anticipated. First, owing to the significantly smaller mean crystallite size in S2 as compared to S1 (see table 1), the density of grain boundary regions in S2 is much larger. This means that electrons in conduction states will have larger scattering, implying a lower mobility and hence a smaller PC. Another possible reason is related to the larger RMS roughness of S2 as compared to S1 (12 nm versus 6 nm, see table 1) and the coarser lateral morphology (characteristic lateral length of 300 nm versus 40 nm) that result from the different growth conditions. This coarse morphology of S2 is indicative of density heterogeneities which could result in high and low photoconductive regions, the overall photoconductance being determined by the connectivity

(percolation) of the high PC regions, as proposed earlier for amorphous silicon [32]. The low photoconductive regions in S2 could also be associated with the high rutile phase component in this sample (see table 1) and the much larger electron effective mass in rutile than in anatase [17]. A third possibility concerns a recently proposed filamentary model that assumes Lévy statistics of waiting times [33] to explain transient resistivity, noise and memory effects in poorly interconnected nanocrystal thin films. Interestingly enough, the observed and predicted transients can also be described by power-law time decay and by intermittently conducting filaments that exhibit current pulses [33]. The fluctuating current behaviour superimposed on a power-law time decay reported here for S2 could be evidence of such a mechanism where the overall current of all filaments does not self-average completely. This picture is particularly interesting as it would provide, if confirmed, an adequate framework to describe PC transients, current fluctuations and resistance switching [13] effects observed in these samples. Clearly, more work is needed, and is under way, to elucidate the connection between the film microstructure and charge transport and phototransport in these nanocrystalline TiO_2 films.

5. Conclusion

We have studied the sub-band-gap excited PC time decay in rf-sputter deposited nanocrystalline TiO_2 thin films. The samples exhibit persistent PC behaviour which we ascribe to slow emission of holes from traps at grain boundaries with energies about 0.85–0.87 eV above the valence band edge. The PC decay after switching off the light source can be well represented by a function that is nearly constant for short times and decreases as a power law for long times (equation (1)). This function has been shown to be consistent with a rate equation characterized by a lifetime that increases linearly with time (equation (3)). This behaviour is consistent with a model that invokes electron and hole spatial separation due to excess-charge-dependent potential barriers at interfaces between grain boundaries and inhomogeneities [10]. This result is expected to have important implications on attempts to determine distributions of trap energies from PC decay curves in nanocrystalline TiO_2. Low absolute PC values observed in a disordered film deposited at a relatively low substrate temperature are tentatively attributed to low electron mobilities due to either large scattering at grain boundaries or poor connectivity of spatially separated photoconductive regions.

Acknowledgments

This work has been partially funded by the Argentinean agencies CONICET, CIUNT (grant E328) and FONCyT (PICT and PICTR20770). We are indebted to Professor Monica Cotta for access to the atomic force microscope.

Appendix

S–S [10] assume that the recombination and drift of excess electrons in a heterogeneous semiconductor are limited by potential barriers E_{rec} and E_{dr}, both being decreasing functions of the carrier density (n): $E_{\mathrm{rec}} = An^{-\alpha}$ and $E_{\mathrm{dr}} = Bn^{-\beta}$, where A, B, α and β are constants. Their main result is an 'instantaneous' relaxation time of the conductivity that is a linear function of time:

$$\tau_{\mathrm{inst}} \equiv \frac{\sigma}{\left|\frac{\mathrm{d}\sigma}{\mathrm{d}t}\right|} = \frac{t + C}{\frac{kT}{A}\left(\frac{B}{kT}\right)^{\alpha/\beta}}, \tag{A.1}$$

where σ is the experimental conductivity and C is a constant. Using S–S's definition (A.1) to calculate the relaxation time from our equation (1), we find that

$$\tau_{\text{inst}} = (b\gamma)^{-1} + \left(\frac{t}{\gamma}\right) = \tau \tag{A.2}$$

i.e. τ_{inst} and τ are equivalent. From (A.1) and (A.2), the relation between the phenomenological constants b and γ and S–S's model parameters can be found:

$$\gamma = \frac{kT}{A}\left(\frac{B}{kT}\right)^{\alpha/\beta} \tag{A.3}$$

and

$$b = C^{-1}. \tag{A.4}$$

References

[1] Mohammadi M R, Cordero-Cabrera M C, Fray D J and Ghorbani M 2006 *Sensors Actuators* B **120** 86
[2] Barnes M C, Gerson A R, Kumar S and Hwang N-M 2004 *Thin Solid Films* **446** 29
[3] Anta J A, Nelson J and Quirke N 2002 *Phys. Rev.* B **65** 125324
[4] Zhou J-H and Elliott S R 1992 *Phys. Rev.* B **46** 12402
[5] Shimakawa K, Murata K, Matsunomo S and Naito H 2006 *J. Non-Cryst. Solids* **352** 1671
[6] Lee C H, Yu G and Heeger A J 1993 *Phys. Rev.* B **47** 15543
[7] Studenikin S A, Golego N and Cocivera M 1998 *J. Appl. Phys.* **84** 5001
[8] Moazzami K, Murphy T E, Phillips J D, Cheung M C-K and Cartwright A N 2006 *Semicond. Sci. Technol.* **21** 717
[9] Xie Z, Burkalov V M, Henry B M, Kirov K R, Smith H E, Grovenor C R M, Assender H E, Briggs G A D, Kano M and Tsukahara Y 2006 *Phys. Rev.* B **73** 113317
[10] Sheinkman M K and Shlik A Ya 1976 *Sov. Phys.—Semicond.* **10** 128
[11] Comedi D, Villafuerte M, Juárez G and Heluani S P 2006 *ECS Trans.* **3** 135
[12] Heluani S P, Comedi D, Villafuerte M and Juarez G 2007 *Physica* B **398** 305
[13] Villafuerte M, Juárez G, Heluani S P and Comedi D 2007 *Physica* B **398** 321
[14] Swanepoel R 1983 *J. Phys. E: Sci. Instrum.* **16** 1514
[15] Glassford K M and Chelikowsky J R 1992 *Phys. Rev.* B **46** 1284
[16] Thornton J A 1974 *J. Vac. Sci. Technol.* **11** 666
[17] Tang H, Prasad K, Sanjinès R, Schmid P E and Lévy F 1994 *J. Appl. Phys.* **75** 2042
[18] Ghosh A K, Wakim F G and Addiss R R Jr 1969 *Phys. Rev.* **184** 979
[19] Yu N and Halley J W 1995 *Phys. Rev.* B **51** 4768
[20] Street R A 1991 *Hydrogenated Amorphous Silicon* (New York: Cambridge University Press)
[21] Werner J and Peisl M 1985 *Phys. Rev.* B **31** 6881
[22] Könenkamp R 2000 *Phys. Rev.* B **61** 11057
[23] Forro L, Chauvet O, Emin D, Zuppirolli L, Berger H and Lévy F 1994 *J. Appl. Phys.* **75** 633
[24] Monroe D 1985 *Phys. Rev. Lett.* **54** 146
[25] Scher H and Montroll E W 1975 *Phys. Rev.* B **12** 2455
[26] Bisquert J 2003 *Phys. Rev. Lett.* **91** 010602
[27] van de Lagemaat J, Kopidakis N, Neale N R and Frank A J 2005 *Phys. Rev.* B **71** 035304
[28] Sanjinés R, Tang H, Berger H, Gozzo F, Margaritondo G and Lévy F 1994 *J. Appl. Phys.* **75** 2945
[29] Plugaru R, Cremades A and Piqueras J 2004 *J. Phys.: Condens. Matter* **16** S261
[30] Montoncello F, Carotta M C, Cavicchi B, Ferroni M, Giberti A, Guidi V, Malagù C, Martinelli G and Meinardi F 2003 *J. Appl. Phys.* **94** 1501
[31] Grunes L A, Leapman R D, Wilker C N, Hoffmann R and Kunz A B 1982 *Phys. Rev.* B **25** 7157
[32] Lust L M and Kakalios J 1995 *Phys. Rev. Lett.* **75** 2192
[33] Novikov D S, Drndic M, Levitov L S, Kastner M A, Jarosz M V and Bawendi M G 2005 *Phys. Rev.* B **72** 075309